JOURNAL GEOLOGICAL SOCIETY OF INDIA
Vol.90, December 2017, pp.769-775

Magnetic Mineralogical Variability along Deccan Trap Basalt Borehole (KBH07), Koyna Deep Continental Drilling Program, Western Maharashtra, India

S. J. Sangode[1*], M. Venkateshwarulu[2], Rasika Mahajan[1] and Vinay Randive[1]

[1]Department of Geology, Savitribai Phule Pune University, Pune - 411 007, India
[2]CSIR-National Geophysical Research Institute, Hyderabad - 500 007, India
******E-mail*: sangode@rediffmail.com

ABSTRACT

A 1248 m long core (KBH 07, 17°18'07" N; 73°47'28.2"E, 960m above msl) drilled up to basement in the Deccan traps from Koyna region was sampled at ~10m interval for magnetic mineralogical studies. Analysis of routine rock magnetic parameters (mass specific magnetic susceptibility: χ_{lf}, frequency dependence of susceptibility: χ_{fd}, susceptibility of anhysteretic remanance: χ_{ARM}, saturation isothermal remanance: SIRM, remanance coercivty: $B_{(0)CR}$, $Soft_{IRM}$, $Hard_{IRM}$, S-Ratio, SIRM/χ_{lf}, χ_{ARM}/χ_{lf}) and density (σ, gm/cc) depicted significant higher order temporal variation. The χ_{lf} varies between 13 and 309 x 10^{-8} m^3/kg and is independent of density variation. The χ_{ARM}, $B_{(0)CR}$ and S-Ratios indicate majority of SD-PSD ferrimagnets with episodes of MD ferrimagnetic concentration and few hard coercivity components. The giant plagioclase lath bearing (GPB) horizons show highest variability of ferrimagnetic concentration marked by anomalous peaks. Overall the variability of rock magnetic parameters independent of lava flow units suggest that the changeover in magnetic mineral concentration, composition and domain size occur at major episodes in magma composition (e.g., primary source, crustal contamination and fractional crystallization). The studied parameters are therefore examined to mark intervals of (i) magma compositional changes, (ii) zones of oxidative conditions and (iii) rapid/slow cooling intervals demanding detailed petrologic studies. We identified one I order trend, four II order cycles and eight III order cycles for the purpose of correlation. Notable peak in χ_{lf} at 650-700m, the changeover in rock magnetic parameters at ~930 m and ~280 m can facilitate marker intervals while several higher order variations can be adopted for high resolution correlation to other boreholes in the region. The complex variation in rock magnetic parameters independent of flow units reflect temporal magnitudes of compositional variability, cooling and emplacement history that needs detailed petro-mineralogical attempts; and the present data is useful for high order inter-core correlations under the deep drilling program.

INTRODUCTION

Several attempts on the correlation of basaltic magma flows in the Deccan volcanic province were made based on mapping, magnetostratigraphy, mineralogy and chemostratigraphy at various orders that are discussed by earlier workers (Cox and Hawkesworth 1985; Beane et al., 1986; Lightfoot et al., 1990; Mitchell and Widdowson, 1991; Peng et al., 1994; Peng 1998; Subbarao et al. 1988; 1994; 2000). The Deccan trap tholeiitic lava flows have been generally classified into three sub-groups and twelve formations recognized by simple field observations that are later improved using isotope, major and trace element geochemistry (e.g. Mahoney, 1988; Beane et al., 1986; Devey, 1986, Mitchell and Widdowson, 1991; Peng et al., 1994). Mapping and magneto-stratigraphy provided fundamental first order tool (e.g., Chenet et al 2008) to decipher the chronologic order at subgroup and formation level; while geochemical ratios lead to higher order information (e.g., Peng et al., 1998). These approaches however are time consuming and expensive compared to the rapid methods like rock magnetism having several advantages in ferrimagnetically rich assemblage of the Deccan basalt.

The Deccan basalts comprises titanomagnetite rich magnetic mineralogy; unequivocally providing higher order resolution for rock magnetic analysis surpassing instrumental noise (Radhakrishnamurty and Likhite, 1970; Radhakrishnamurty and Deutsch, 1974; Radhakrishnamurty and Subbarao, 1990; Radhakrishnamurty et al., 1977; 1990; Chenet et al., 2008; Sangode et al., 2017). The strong ferrimagnetism of Deccan basalts is unimodally contributed by the titanomagnetite (TM) solid solution series. TM is an important mineralogical indicator for lava compositional and cooling history; and the Ti- substitution in TM alters the Curie temperatures and many other rock magnetic properties (Radhakrishnamurty and Likhite, 1970; Radhakrishnamurty and Deutsch, 1974; Radhakrishnamurty et al., 1977, 1981; Radhakrishnamurty and Subbarao, 1990; Dunlop and Ozdemir, 1997; Chenet et al., 2008; Sangode et al., 2017). Titanomagnetite is an intermediate member of the isomorphous series of solid solutions of magnetite ($FeFe_2O_4$, ferrimagnetic), ulvospinel (Fe_2TiO_4, paramagnetic), and magnesian ulvospinel (Mg_2TiO_4). Titanomagnetites occur as octahedral crystals and can contain substitutes like Al^{3+}, V^{4+}, Gr^{3+} and Mn^{2+} and commonly occur as granular aggregates when observed under ore microscope. The density of TM lies between 4,800 to 5,300 kg/m^3 and its Curie points show systematic variation from 0°–100°C (for ulvospinel with $FeFe_2O_4$ content up to 20 %) to 500 to 570°C (for magnetite with Fe_2TiO_4 content up to 10 %).

The Deccan lava comprises Fe-rich peridotitic source with small volumes of alkalic or transitional magma (Sen, 1995; Melluso et al., 2006; Sheth and Melluso 2008) and therefore shows close association of Fe- bearing minerals to other petrological components. The Deccan primary magma generation is reported to have evolved with great variation in SiO_2 and Al_2O_3 and other components of crustal contamination. Under these conditions the role of Ti is not well understood demanding more information on the TM series that can be routinely characterized using mineral magnetism (Collinson, 1983; Thompson and Oldfield, 1986; Dunlop and Ozdemir, 1997; Evans and Heller, 2003; Sangode, 2014; Liu et al., 2012; Sangode et al., 2017). Such information may provide significant inputs to understand the titanomagnetite framework and systematics within the magmatic processes of Deccan volcanism with further detailed petrologic attempts.

In absence of any detailed integrated magnetic mineral-petrological information, the present attempt assume at least two primary sources

0016-7622/2017-90-6-769/$ 1.00 © GEOL. SOC. INDIA | DOI:10.1007/s12594-017-0789-2

of change in concentration and composition of TM bearing ferrimagnetic mineralogy marked by (a) compositional changes in the source magma, and (b) the style of cooling in the given lava flow unit. A set of parameters based on the rock/mineral magnetic analysis (accounted in Thompson and Oldfield, 1986; Evans and Heller, 2003; Liu et al., 2012) can therefore provide a routine database to investigate many of the above mentioned aspects on Deccan volcanism apart from its advantage as a rapid, economic tool for stratigraphic core-correlation. With this rationale we attempted the rock magnetic study alongside precise measurement of density in the studied core for its extensive use under the Koyna drilling program, and the Deccan stratigraphy in general.

METHODS

The drilled core of borehole KBH 07 was further subsampled by precisely cutting 2.2 cm slices at various intervals of ~5 to ~18m (average ~10m). These intervals were decided by visual observations of the lava flow units (total 47 units) to succinctly represent each flow. The slices were then brought to laboratory and further drilled perpendicular to obtain cylindrical cores of 2.5 cm diameter and 2.2 cm heights keeping the top and bottom intact. Each cylinder was then measured precisely for its height and diameter using a digital vernier caliper after measuring the weights on well calibrated digital weighing machine to derive the density. The magnetic susceptibility (χ) was measured in six orthogonal directions to assess the bulk ferrimagnetic concentration (Collinson, 1983) by normalizing the anisotropy. The low and high frequency magnetic susceptibilities (i.e. χlf and χhf) were measured at 0.46 and 4.6 kHz frequencies, respectively, using the standard MS2B laboratory sensor of Bartington (UK). The frequency dependent susceptibility ($\chi fd = \chi lf - \chi hf$) and its percentages ($\chi fd\% = [(\chi lf - \chi hf/\chi lf) \times 100]$) were used to detect the ferrimagnetic grains lying at the boundary of superparamagnetic (SP) and single domain (SD) grains. Anhysteretic Remanence Magnetization (ARM) was grown using Magnon AFD-300 a.f. demagnetizer with peak alternating field of 100 mT in presence of a DC bias field of 0.1 mT normalized by the bias field to express as ARM susceptibility (χARM). The χARM is sensitive to SD ferrimagnetic mineral concentration and the ratio of χARM/χlf indicate relative variation in concentration of fine SP and coarse SD magnetic particles in bulk samples.

Isothermal Remanence Magnetization (IRM) was grown in increment forward fields up to 1000 mT and back fields up to -300 mT using an ASC Impulse Magnetizer and remanences were measured using the Molspin spinner magnetometer. The IRM analysis was carried out to estimate concentration and granulometry of ferri- and antiferromagnetic minerals based on the various parameters and ratios (e.g., Liu et al., 2012). The saturation isothermal remanent magnetization (SIRM) was measured at 1000 mT as standard field. The hard isothermal remanent magnetization [$Hard_{IRM} = 0.5 \times (SIRM + IRM_{-300mT})$] parameter is used to estimate the concentration of antiferromagnetic minerals with its sensitivity to hematite. The soft isothermal remanent magnetization parameter [$Soft\text{-}IRM = 0.5 \times (SIRM - IRM_{-20mT})$] was calculated as proxy to indicate concentration of multi domain (MD) ferrimagnetic minerals (Thompson and Oldfield, 1986; Liu et al., 2012). The ratio SIRM/χlf is studied to decipher relative variation in concentration of very fine SP and coarse SD-MD magnetic particles (Liu et al., 2012). The demagnetization parameter S-ratio (IRM_{-100mT}/SIRM) was calculated to quantify the relative abundance of ferrimagnetic and antiferromagnetic minerals within the bulk sample (Thompson and Oldfield., 1986; Evans and Heller., 2003; Liu et al., 2012).

RESULTS AND DISCUSSION

Table 1 presents the routine rock magnetic parameters at each sampled interval of the KBH 07 borehole. Routine statistics were applied to describe the data. The density shows a mean value of 2.94 gm/cc (n = 112) with median of 2.98 varying within a range from 2.02 to 3.21. The anomalous low values (2.02 and 2.17) in two samples are due to vesicular filling. This indicates fairly large variation in density within the Deccan basalt composition of the Koyna region. The mass specific susceptibility (χ_{lf}) showed a mean value of 96.37 (10e-8 m^3/kg) and a median of 89.64 varying within a range from 13.53 to 308.83 with several anomalous minimum and maximum values. The mean SIRM showed a value of 18037 (10e-5 Am^2/kg) varying from 1943 to 31267 depicting high ferrimagnetic concentration with a large variability. A mean χ_{ARM} of 2.98 (10e-8m^3/kg) varying between 1.08 and 7.97 indicate the high concentration of single domain (SD) grains or high stable remnance. The mean coercivity of remanance ($B_{(0)CR}$) of 32.76 mT varying between 4 and 83 depict majority of SD-PSD grains with presence of MD ferrimagnets and the antiferromagnets.

Figures 1a, b and c presents the data of studied rock magnetic parameters plotted against depth of the core KBH 07. The grey colored straight line over each plot represent the linear trend/regression adopted here as first order trend/variability for each parameter. The grey colored smooth curves (segments) are drawn as iterative curves discarding the anomalous peaks/drops to derive the second order trend marked by cycles (IIa..d) bound by blue bars. The third order cycles are represented by IIIa…h defined by yellow bars. The first order trend line show only fairly increasing or decreasing orders for the entire length of each parameter with the given scale. The density shows an increasing upwards trend in contrast to the decreasing trends of χ_{lf} and SIRM. Although anomalous low density samples are observed in the upper part, the lower part shows some notable trend of low density.

The densities of lava can have several controls, reflecting on the dynamic densities of the magma during fractionation, volatiles contents and the cooling history (Sparks and Huppert, 1984). Since there is no first/second order correlation between density and any other rock magnetic parameter, it appears to have an independent control variously governed by the above processes. Further, it also shows variation independent of the lava flow units depicting its control by magmatic processes rahter than in-situ cooling history. The higher order variability (100's of meter scale shown by the grey segmented peak curves in Fig.1) indicates positive and negative correlations with magnetic susceptibility and other rock magnetic parameters in different segments. Overall the lower part (~1000-1200m) shows an inverse correlation, while the upper part depicts positive correlation with some smaller segments of χ_{lf}. The density is however independent of any of the major peaks in χ_{lf} during 600-700m. Density at this scale of the Koyna core representing >1000m of the stacked lava pile is therefore a reflection of the fractionation and residue history of source magma. This demands a detailed petro-mineralogical and geochemical approach which is beyond the scope of the present attempt. The first order trend between χ_{lf} and SIRM matches while the higher order trend shows only a fair positive correlation (R^2~0.55) with no visible correlative trends at segmental level.

The major peaks in χ_{lf} do not explicitly match with the SIRM. The two magnetic mineral concentration- dependent parameters (χ_{lf} and SIRM) often have obvious positive correlation in ferrimagnetically dominated mineralogy. However the above relation can be explained by possible ferrimagnetic substitutions in other minerals (olivine, pyroxenes etc) that might get saturated under high fields of SIRM. The second order trends in SIRM (shown by the grey segment lines/ peak curves in fig. 1) can therefore be related to magmatic processes yet to be investigated. The frequency dependence of susceptibility (χ_{fd}%) varies below 2% indicating the absence of SP fraction excepting few anomalous peaks corresponding to drop in SIRM

Table 1. The rock magnetic data for the standard parameters from each sampled interval of the KBH 07 core. The flows (F*) marked are based on tentative observations from the core while sampling. The units are: $\chi lf = 10^{-8}\ m^3\ kg^{-1}$, $\chi_{ARM} = 10^{-8}\ m^3\ kg^{-1}$, $B_{0(CR)}$ = mT and for SIRM, Soft-IRM and HIRM = $10^{-5}\ Am^2\ kg^{-1}$, M: massive, B: brecciated, MR: massive reddish coloured, Pl-R: randomly oriented plagioclase laths, Pl<: plagioclase lath density decreased, Pl-0: very small laths, GPB: giant plagioclase basalt. L.N.: Lab number, F*: observed flow unit, Fc: flow characters, D: depth in meters, σ: density = gm/cc.

L.N.	F*	Fc	D	σ	χlf	χfd%	SIRM	χ_{ARM}	Soft IRM	Hard IRM	$B(0)_{CR}$	S-Ratio	SIRM/χlf	X_{ARM} χlf
1	F1	M	33.03	2.98	75.02	0.58	27159	2.75	3728	7.27	46	-0.90	362	36.65
2	F1	M	38.77	3.03	35.89	1.08	11829	2.96	9422	0.00	11	-0.98	330	82.47
3	F1	M	42.26	3.00	68.34	0.36	14526	1.45	4338	89.85	33	-0.81	213	21.21
4	F2	M	52.30	2.98	35.51	0.98	11241	2.69	9020	0.00	11	-0.98	317	75.83
5	F2	M	57.89	3.08	49.66	0.62	13590	2.88	8938	18.84	19	-0.92	274	58.00
6	F2	M	66.85	3.04	48.27	0.36	5154	1.40	4388	36.50	10	-0.98	107	29.09
7	F2	M	76.76	2.97	54.00	0.42	9387	1.57	5916	0.00	17	-0.98	174	28.99
8	?	M	84.62	2.96	105.72	1.15	22515	3.23	7709	0.00	28	-0.96	213	30.52
9	F3	M	99.51	2.95	90.57	0.77	10664	1.78	6945	0.00	15	-1.00	118	19.63
10	F3	M	107.53	3.00	67.53	0.69	18653	2.98	18621	0.00	7	-1.00	276	44.12
11	F4	M	120.06	3.00	58.19	0.64	18399	3.88	17632	0.00	13	-1.00	316	66.75
12	F5	M	124.83	2.92	86.65	0.57	13342	2.94	10956	0.00	11	-1.00	154	33.94
13	F5	M	134.96	2.85	36.74	0.74	16525	4.00	11582	0.00	16	-0.99	450	108.92
14	F5	M	148.50	3.08	50.84	1.09	12501	3.63	9972	0.00	10	-0.99	246	71.31
15	F5	M	157.36	3.07	40.92	0.71	20068	5.57	11272	0.00	18	-0.91	490	136.19
16	F5	M	168.20	3.09	79.40	5.08	8793	4.10	7862	0.00	5	-1.00	111	51.65
17	F5	M	180.05	3.13	76.08	3.26	8315	3.17	7201	0.00	4	-0.99	109	41.73
18	F6	M	186.83	2.80	133.69	0.24	24734	4.42	1000	0.00	36	-0.98	185	33.07
19	F6	M	194.26	2.97	117.71	0.20	22552	2.43	3647	0.00	44	-0.74	192	20.62
20	F6	M	202.44	2.84	79.48	0.74	21348	2.28	2711	15.58	48	-0.99	269	28.70
21	F7	M	210.89	3.02	131.28	0.29	22358	2.66	5834	535.01	35	-0.80	170	20.29
22	F7	M	220.57	2.95	86.24	0.63	15530	4.13	13241	248.62	4	-0.97	180	47.88
23	F7	M	225.46	3.00	130.26	0.58	18738	4.42	14386	316.68	16	-0.95	144	33.92
24	F8	M	242.88	3.14	157.36	0.16	15232	1.58	5222	307.91	35	-0.83	97	10.02
25	F8	M	250.18	2.97	105.31	0.82	24064	3.45	3394	386.82	46	-0.74	229	32.80
26	F8	M	256.91	2.99	86.20	0.20	18831	2.05	5467	129.11	32	-0.88	218	23.84
27	F8	M	266.29	2.98	87.86	0.35	18321	2.31	5691	104.62	31	-0.90	209	26.32
28	F8	M	276.67	3.12	100.72	0.51	20152	2.74	6566	83.24	29	-0.93	200	27.25
29	?	M	284.39	3.02	124.41	0.51	17411	2.41	6741	109.70	25	-0.94	140	19.38
30	F9	M	287.49	2.71	14.34	7.65	1943	6.62	165	389.48	77	-0.23	136	461.74
31	F9	M	306.47	2.74	14.91	1.96	8949	4.85	487	506.46	83	-0.18	600	325.11
32	F9	M	312.11	2.87	44.23	0.46	18470	1.82	3163	110.07	42	-0.85	418	41.17
33	F10	M	316.36	2.02	95.81	0.00	11997	2.19	3819	1505.10	38	-0.74	125	22.88
34	F10	M	322.84	2.94	136.05	0.35	24966	2.02	3396	87.93	44	-0.81	184	14.83
35	F10	M	329.93	2.94	73.01	0.16	20073	1.50	3556	207.02	42	-0.79	275	20.61
36	F10	M	339.33	2.95	81.62	0.00	12841	2.33	6762	0.00	18	-0.99	157	28.51
37		M	352.11	3.04	36.22	0.00	8118	4.47	1227	368.69	49	-0.59	224	123.40
38		M	355.09	3.04	47.74	1.07	7498	5.57	1826	392.98	39	-0.67	157	116.64
39	F11	B	362.16	2.94	65.50	0.59	20608	7.94	1745	850.93	74	-0.35	315	121.17
40	F12	M	373.42	2.76	62.67	0.93	29183	1.46	499	141.62	77	-0.44	466	23.23
41	F12	M	378.25	2.17	106.90	0.38	15274	3.46	5069	554.61	26	-0.77	143	32.35
42	F12	M	383.81	2.91	147.57	0.47	22276	2.64	10620	261.57	38	-0.79	151	17.90
43	F12	M	396.99	3.14	128.03	0.32	21920	2.30	5828	306.58	34	-0.87	171	17.95
44	F12	M	406.41	3.00	89.34	0.92	21929	4.15	10156	188.23	22	-0.91	245	46.45
45	F12	M	413.55	3.11	114.00	0.37	23779	3.26	6090	160.80	33	-0.94	209	28.63
46	F13	M	427.98	3.10	96.85	0.32	24650	1.83	2854	5.58	49	-0.77	255	18.91
47	F13	M	440.22	3.12	105.91	0.61	13882	2.93	8529	0.00	15	-0.97	131	27.66
48	F13	M	447.07	3.14	114.84	0.51	23828	2.48	4329	15.90	39	-0.88	207	21.57
49	F14	MR	456.78	2.77	13.53	1.29	4259	4.47	689	380.72	45	-0.61	315	330.30
51	F15	M	484.01	3.11	87.84	0.33	23981	2.43	3683	93.83	43	-0.85	273	27.70
50	F15	M	486.05	2.91	122.33	0.49	27529	3.31	2837	0.00	43	-0.93	225	27.08
52	F16	M	497.41	2.95	115.42	0.53	21792	3.23	1000	40.00	48	-1.00	189	28.02
53	F17	M	504.01	2.94	110.99	0.71	26446	3.66	3311	89.62	41	-0.95	238	33.01
54	F18	M	524.42	3.14	108.49	1.26	12560	4.64	10502	38.06	5	-1.00	116	42.73
55	F19	M	547.30	2.46	81.80	0.72	21244	1.70	3585	383.13	44	-0.77	260	20.79
56	F19	M	555.01	3.07	74.35	0.31	25953	2.74	264	48.47	67	-0.82	349	36.87
57	F19	M	577.14	3.06	98.30	0.30	23700	2.48	4692	155.23	40	-0.89	241	25.27
58	F19	M	603.78	3.21	85.31	0.19	23685	2.00	3826	184.61	39	-0.89	278	23.50
59	F20	Pl-R	616.06	3.03	15.25	6.41	2674	2.32	207	0.00	81	-0.25	175	152.13
60	F20	Pl-R	625.56	3.03	36.35	1.52	10569	7.97	1700	561.12	48	-0.66	291	219.31
61	F21	M	640.53	3.01	183.30	0.39	25346	2.10	5387	80.04	36	-0.93	138	11.44
62	F21	M	651.99	3.06	139.16	0.36	26344	2.37	2699	51.89	43	-0.94	189	17.05
63	F22	M	658.81	2.98	110.85	0.62	15052	1.20	4196	448.03	34	-0.75	136	10.80
64	F23	Pl<	668.53	2.97	308.83	0.12	15725	4.46	1000	0.00	35	-1.00	51	14.44
65	F23	Pl<	680.22	3.01	253.05	0.67	24886	5.12	13207	52.01	18	-0.97	98	20.25
66	F24	Pl<	689.21	3.08	129.52	0.32	24394	2.82	6152	207.72	33	-0.89	188	21.79
67	F24	Pl<	700.55	3.00	119.91	0.39	24126	2.44	5170	180.65	35	-0.90	201	20.31
68	F25	Pl-0	715.98	3.00	26.28	7.84	9913	2.29	7424	55.41	12	-0.99	377	87.23

Table 1. Contd...

L. N.	F*	Fc	D	σ	χlf	χfd%	SIRM	χ_{ARM}	Soft IRM	Hard IRM	$B(0)_{CR}$	S-Ratio	SIRM/χlf	X_{ARM} χlf
69	F25	Pl-0	734.27	3.10	120.21	0.61	22581	2.04	5171	233.63	35	-0.88	188	16.97
70	F26	M	745.49	3.01	108.17	0.14	19120	3.45	1000	0.00	48	-1.00	177	31.91
71	F26	M	749.64	2.95	176.64	0.60	24332	4.07	9803	0.00	25	-0.95	138	23.04
72	F27	M	764.63	3.21	98.94	1.41	12728	3.00	7310	0.00	17	-0.99	129	30.34
73	F28	M	769.27	2.97	109.44	0.18	19869	2.34	6632	0.00	30	-0.92	182	21.37
74	F29	M	786.39	2.99	58.86	0.49	12083	1.08	3141	35.97	35	-0.86	205	18.27
75	F30	M	795.82	2.84	131.02	0.37	12176	2.63	3852	0.00	29	-1.00	93	20.05
76	F31	M	815.84	2.81	68.53	0.90	9211	2.58	5437	0.00	16	-1.00	134	37.68
77	F32	M	831.22	2.85	106.92	0.26	22553	3.01	6987	0.00	30	-0.95	211	28.16
78	F33	M	854.80	3.14	84.14	0.69	15826	3.56	10297	0.00	14	-0.91	188	42.33
79	F33	M	856.77	3.06	83.89	1.35	12279	3.79	10197	0.00	8	-1.00	146	45.22
80	F33	M	883.78	3.15	89.88	1.62	12462	4.55	9975	0.00	7	-0.93	139	50.65
81	F33	M	897.54	3.09	98.31	0.35	12495	2.88	9049	154.43	12	-0.96	127	29.29
82	F34	M	919.14	2.99	100.71	0.95	19712	4.10	10167	146.86	20	-0.94	196	40.71
83	F35	M	934.83	2.90	20.12	11.28	16161	4.82	13074	174.21	10	-0.97	803	239.68
84	F35	M	964.92	3.07	102.28	0.49	25999	3.12	1501	22.41	45	-0.94	254	30.48
85	F35	M	985.39	3.19	107.51	0.28	24601	2.34	3068	216.70	43	-0.87	229	21.72
86	F36	M	1003.22	3.02	76.01	0.58	17842	1.18	3494	519.88	42	-0.72	235	15.55
87	F37	M	1015.28	3.16	71.05	0.58	17377	1.47	3122	463.49	45	-0.69	245	20.68
88	F37	M	1023.48	2.96	99.24	0.55	21882	2.37	5354	323.63	36	-0.86	220	23.88
89	F37	M	1040.72	3.06	127.12	0.69	24674	3.18	5063	322.76	36	-0.88	194	24.98
90	F38	M	1056.10	2.92	138.12	1.04	22611	4.33	9560	261.80	24	-0.93	164	31.35
91	F39	M	1069.92	2.77	60.56	0.42	16003	1.39	3009	268.59	43	-0.75	264	23.03
92	F40	M	1075.08	2.84	86.12	0.96	23106	3.26	3823	513.83	43	-0.73	268	37.82
93	F41	M	1084.19	2.85	63.04	0.23	12356	1.29	4161	232.90	30	-0.83	196	20.42
94	F42	M	1098.86	2.76	111.88	0.17	10670	2.30	5830	106.92	18	-0.94	95	20.55
95	F43	M	1104.01	2.57	99.13	0.30	21161	2.32	5179	271.52	35	-0.88	213	23.38
96	F43	M	1115.41	2.80	77.68	0.75	14380	1.36	3868	314.41	35	-0.81	185	17.49
97	F44	M	1123.61	2.89	76.66	0.53	7884	2.11	5389	-7.98	13	-0.99	103	27.48
98	F45	M	1138.51	2.94	126.26	0.39	24754	3.18	7748	395.41	31	-0.88	196	25.21
99	F45	M	1148.24	2.86	106.05	0.53	19827	1.75	5603	369.80	43	-0.86	187	16.51
100	F45	M	1158.16	3.04	187.92	0.45	26197	3.20	5742	345.69	35	-0.93	139	17.02
101	F45	M	1167.93	2.96	170.93	0.35	15349	1.91	6641	205.61	24	-0.86	90	11.20
102	F46	M	1173.08	2.89	76.62	0.32	21280	1.40	1000	241.32	47	-0.70	278	18.23
103	F46	M	1179.60	2.76	76.71	0.38	21851	1.28	3583	315.48	45	-0.74	285	16.70
104	F46	M	1190.66	2.76	79.31	0.21	19295	1.54	4286	241.81	39	-0.75	243	19.35
105	F46	M	1195.01	2.74	80.00	0.27	18422	1.43	4124	250.01	40	-0.79	230	17.83
106	F46	M	1211.22	2.84	89.40	0.23	15460	1.59	5661	110.76	28	-0.84	173	17.75
107	F46	M	1217.35	2.70	67.42	0.22	14661	1.19	3563	190.82	38	-0.78	217	17.59
108	F46	GPB	1222.71	2.92	37.93	0.70	5895	5.38	1361	277.89	44	-0.60	155	141.79
109	F47	GPB	1232.01	3.00	126.65	0.81	28555	2.32	2498	48.95	52	-0.72	225	18.31
110	F47	GPB	1237.48	2.54	266.46	0.36	31268	6.64	3402	0.00	37	-1.00	117	24.91
111	F47	GPB	1240.00	2.84	167.16	0.33	18583	2.99	8200	151.63	23	-0.84	111	17.91
112	F47	GPB	1247.77	2.55	186.60	1.57	30400	4.30	6129	0.00	35	-0.93	163	23.06

related to paleo- weathered zones observed in the drilled core.

The χ_{ARM} show a general negative correlation with SIRM and suggest that the SIRM is influenced by minerals other than SD ferrimagnets and also possibly substitutes in other minerals like pyroxene or olivine as stated above needing further investigation. The $Soft_{IRM}$ show different trends (variability) with some peaks matching to χ_{ARM}. The coercivity of remanance ($B_{(0)CR}$) show segments dominated by SD (Single domain~ and MD (multi domain) size. The MD size can be assigned to relatively larger time available for crystallization compared to that of rapid crystallizations in SD ferrimagnets. The S-Ratio broadly matches with $B_{(0)CR}$ depicting the MD-PSD-SD ferrimagnetic distribution with some anomalous peaks of harder ferrimagnets or the mixture of ferri and antiferromagnets indicating oxidative conditions. The SIRM/χ_{lf} and χ_{ARM}/χ_{lf} matches each other with several anomalous peaks depicting the high/low concentration of SD ferrimagnets, but with overall dominance of SD ferrimagnets depicting relatively faster cooling history.

From the above results, we derive several events of broad changes in the form of (i) unknown magma composition cycles, (ii) zones of oxidative conditions and (iii) zones of rapid/slow cooling that are displayed in the Fig.1. We also discuss the limitations of making these assumptions from a single core data which needs representation from additional data to test the lateral extent. Similar such attempts are therefore needed with adjacent cores apart from detailed petrological (microscopic) studies. The anomalous peaks/drops in the rock magnetic results therefore may represent such sampling bias and therefore we presented the iterative curve segments to infer the second and third order cycles (II and III in the Fig.1).

The top and bottom parts of the flow anticipate faster cooling and may form fine grained ~TM60 with associated low Curie and unblocking temperatures. The slower cooled central part of the flow pertains better unmixing into the magnetite and ulvospinel end-members yielding coarse-grained magnetite lamella (~TM0) with high Curie and unblocking temperatures. The magnetic mineralogical variation independent of the flow units therefore suggested dominance of magmatic processes over lava flow emplacement.

The growth of large phenocrysts (GPB) need sufficient time and suggested to have been equal to the eruption time of the formation they belong and crystallized in convecting, upper crustal magma chambers (Hooper et al., 1988; Sen, 2001; Borges, 2007; Michael and Chandrasekharam, 2007; Borges et al., 2013). Being buoyant, they are accumulated near the top of magma chamber and increase in size in response to the continuous supply of magma. Pulse of high viscosity ferrimagnetic magma may have released the GPB (op. cit.)

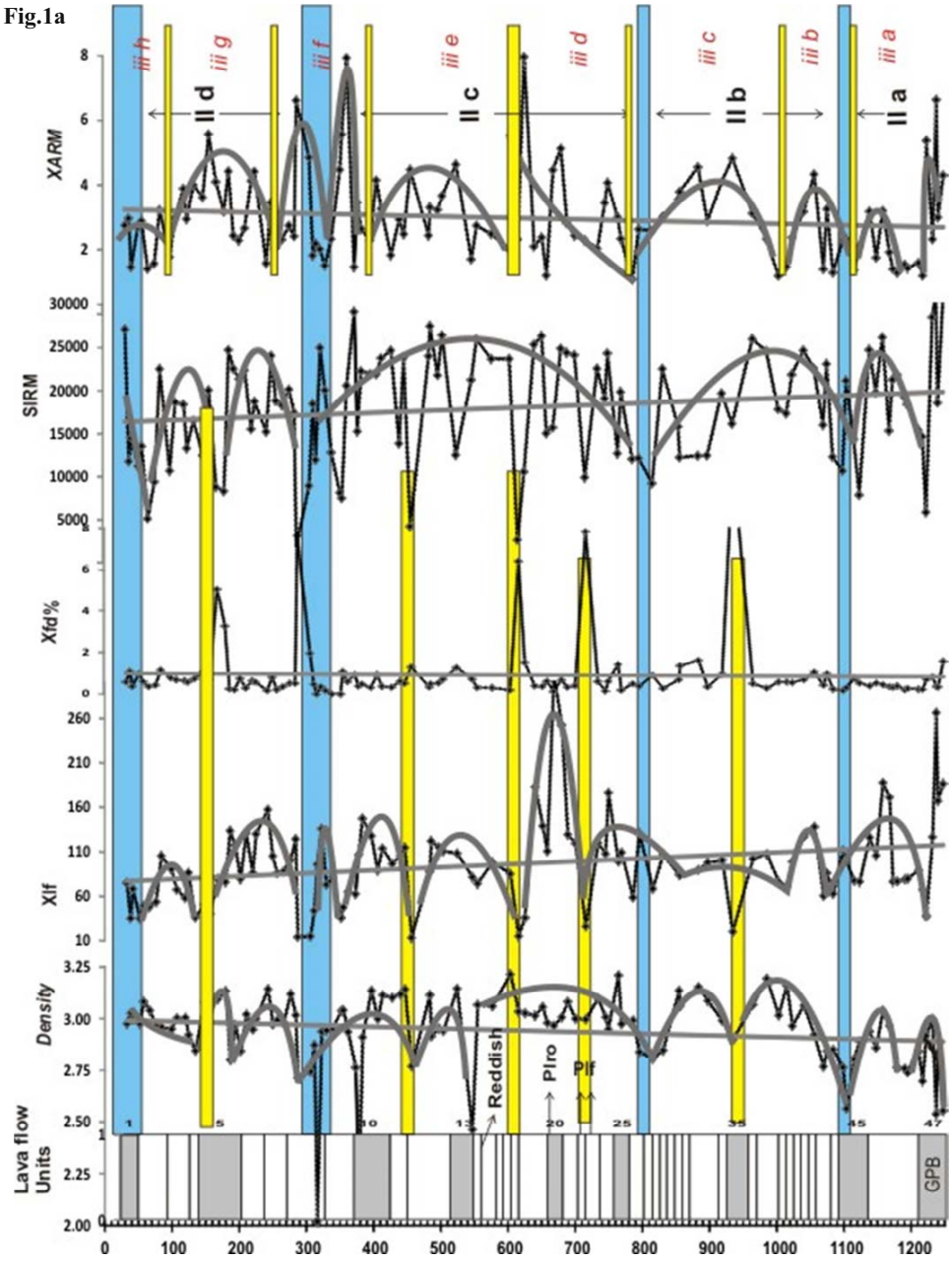

Fig.1a, 1b & 1c: The fundamental rock magnetic parameters and their ratios (the data plot in black dotted lines) are plotted with depth of the core in meters. The straight grey line subparallel to the depth axis in each plot represents the linear first order trend. The grey colored smooth bell-shaped curves (/segments) are drawn as iterative curves (normalizing the anomalous peaks/drops) to derive the second order cycles (IIa..d), separated by blue bars. The third order cycles are represented by IIIa…h separated by yellow bars. Details on variation are discussed in the text.

resulting into the anomalous peaks in ferrimagnetic concentration at these intervals.

As stated above the χ_{lf} is controlled by ferrimagnetic minerals of TM series, while the SIRM imparting a high field is governed by ferri and antiferromagnetic assemblages as inclusions in various other minerals including the Fe-rich olivine; apart from the TM. This is evident from the absence of correlation between χ_{lf} and SIRM, which otherwise should correlate significantly. Considering this, we relied upon SIRM as larger representative of the petrological compositions. The second order cycles shown by SIRM (IIa, b, c & d in Fig. 1) therefore appears to be more representative for the magmatic compositional cycles. These cycles are then explained by comparison to other rock magnetic parameters. The cycle IIa comprises GPB with distinct peak in SIRM and large fluctuation in other parameters. The GPB representing feldspars record low ferrimagnetic concentration while the matrix basalt is highly ferrimagnetic resulting into the fluctuations. The second cycle IIb shows a peak in SIRM and the twin peaks of χ_{ARM}, SoftIRM and SIRM/χ_{lf}. This cycle is therefore divided into sub-cycles as third order variation (III in Fig.1). This interval shows three saw-toothed peaks of SIRM/χ_{lf} depicting ferrimagnetic cycles followed by bell shaped peaks matching with the succeeding third order cycles.

The third megacycle (IIc) can be divided into few higher order cycles. The χ_{ARM} show major peaks depicting faster/slower cooling rates. The IIc also contains a major peak in χ_{lf} without any change in χ_{fd} but drop in χ_{ARM} thus indicating rise in MD ferrimagnetic concentration to depict slower cooling rates. The fourth megacycle (II d) marks at least two-III order cycles of changes in domain size within the ferrimagnetic mineralogy. The HardIRM that may represent oxidative conditions due to antiferromagnetism shows three independent cycles.

The above description indicated complex magnetic mineralogical

Fig.1b

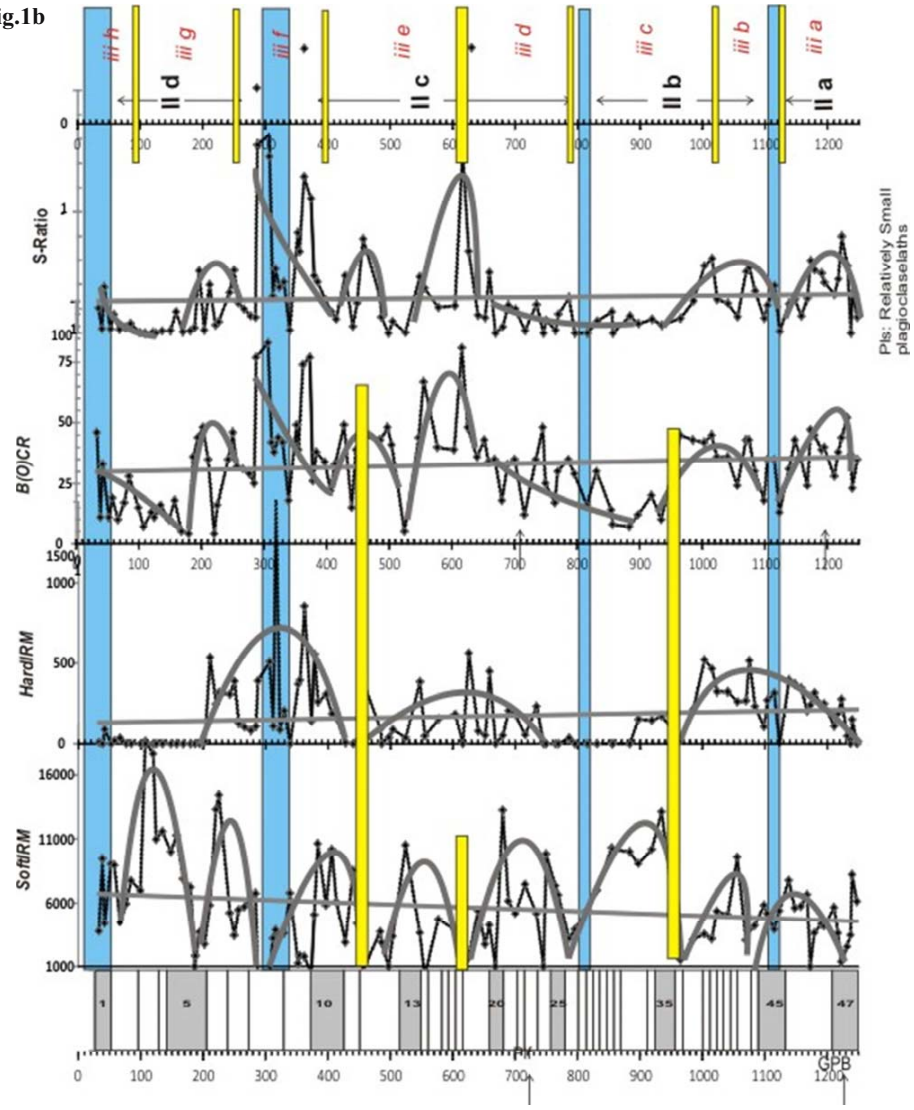
iii h
iii g
iii f
iii e
iii d
iii c
iii b
iii a
II d
II c
II b
II a
S-Ratio
B(O)CR
HardIRM
SoftIRM
Pls: Relatively Small plagioclaselaths
GPB

Fig.1c

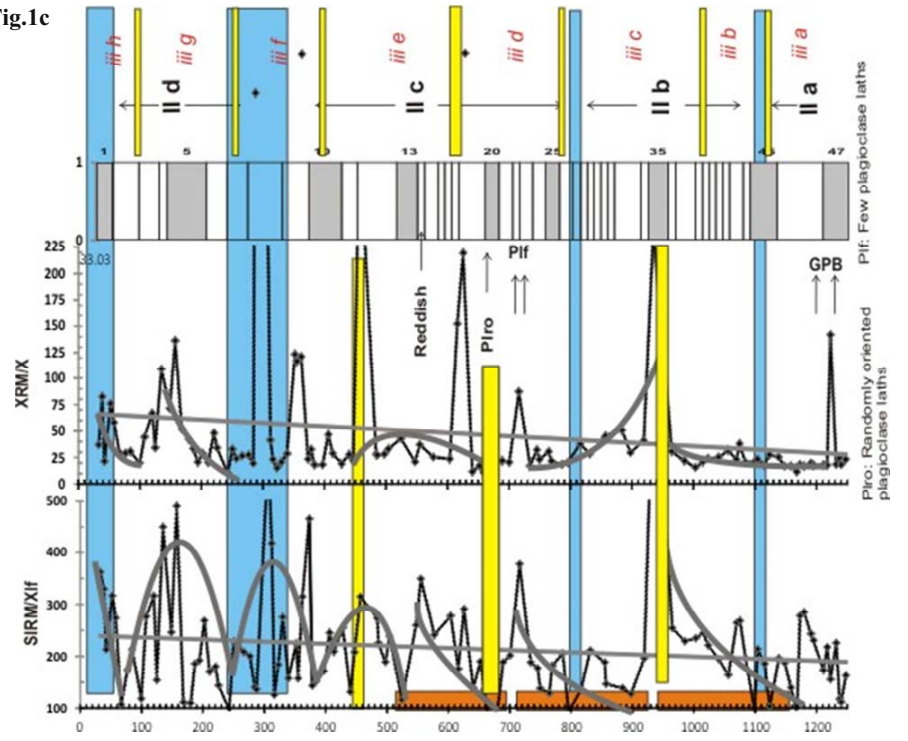
iii h
iii g
iii f
iii e
iii d
iii c
iii b
iii a
II d
II c
II b
II a
XRM/X
SIRM/Xlf
Reddish
Plro
Plf
GPB
Plf: Few plagioclase laths
Plro: Randomly oriented plagioclase laths

variation which is very useful to decipher various magmatic-, mineralogical processes and cooling rate changes. However, the present approach needs to be established and calibrated with detailed petro-mineralogical and geochemical studies to describe the changes. Further, such an attempt on additional cores with same instrumental setup will create a robust database to establish the magnetic stratigraphy and understand some of the magmatic processes in Deccan volcanism.

CONCLUSION

The present attempt on Deccan basalt core KBH07 demonstrated a good variability amongst the rock magnetic parameters for its application as an efficient correlative tool under Koyna drilling program. The study decipher a complex magnetic mineralogical variation independent of the physical lava flow units suggesting its control by magmatic/mineralogical and/or cooling style related changes. The variability amongst these parameters (including density), independent of individual lava flow unit suggesting their relation to magmatic compositional trends further demand detailed petro-mineralogic and geochemical studies to enhance the utility of the studied rock magnetic signatures. The study anticipates developing robust database to understand the stratigraphy and evolutionary processes by analysis of additional cores in the region.

Acknowledgements: We acknowledge the generous funding and facilities provided under the Ministry of Earth Science, New Delhi under the grant MoES/P.O.(Seismo)/1(180)/2013. Encouragement from Dr H.K. Gupta and Dr B.K. Bansal, and the support at BGRL from Dr Sukanto Roy is greatly acknowledged. The laboratory facility at Department of Geology, SPPU under DST-FIST program is acknowledged. We are thankful for critical reviews by two anonymous referees that greatly improved the manuscript. Director, CSIR-NGRI, Hyderabad and Head, Dept. of Geology SPPU are acknowledged for support, permissions and facilities to accomplish the work.

References

Beane, J.E., Turner, C.A., Hooper, P.R., Subbarao, K.V. and Walsh, J.N. (1986) Stratigraphy, composition and form of the Deccan Basalts, Western Ghats, India. Bull. Volcanol., v.48, pp.61-83.

Borges, M.L. (2007) Life Cycle of Deccan Trap Magma Chambers: A Crystal Scale Elemental and Strontium Isotopic Investigation. Ph.D. Dissertation, Florida International University, Miami, USA. 165p.

Borges, M.R., Sen, G., Hart, G.L., Wolff, J.A., Chandrasekharam, D. (2013) Plagio-clase as recorder of magma chamber processes in the Deccan Traps: Sr-isotope zoning and implications for Deccan eruptive event. Jour. Asian Earth Sci., v.84, pp. 95-101. DOI: 10.1016/j.jseaes.2013.10.034.

Chenet, A.-L., Fluteau, F., Courtillot, V., Gérard, M. and Subbarao, K.V. (2008) Determination of rapid Deccan eruptions across the Cretaceous-Tertiary boundary using paleomagnetic secular variation: Results from a 1200-m-thick section in the Mahabaleshwar escarpment. Jour. Geophys. Res., v.113, B04104.

Collinson, D.W. (1983) Methods in Rock Magnetism and Palaeomagnetism: Techniques and Instrumentation. Chapman and Hall, New York, 503p

Cox, K.G. and Hawkesworth, J. (1985) Geochemical Stratigraphy of the Deccan Traps at Mahabaleshwar, Western Ghats, India, with Implications for Open System Magmatic Processes. Jour. Petrol., v.26, pp.355-377.

Devey, C.W. and Lightfoot, P.C. (1986) Volcanological and tectonic control of stratigraphy and structure in the western Deccan Traps. Bull. Volcanol., v.48, pp.195–207.

Dunlop, D.J. and Ozdemir, O. (1997) Rock magnetism, Fundamentals and frontiers. Cambridge Studies in Magnetism Series. xxi+573p. Cambridge.

Evans, M.E. and Heller, F. (2003). Environmental Magnetism: Principles and Applications of Enviromagnetics. Academic, San Diego, California. 311p.

Hooper, P.R., Subbarao, K.V. and Beane, J.E. (1988) The giant plagioclase basalts (GPBs) of the Western Ghats, Deccan Traps. Mem. Geol. Soc. India, no.10, pp.135–144.

Lightfoot, P., Hawkesworth, C., Devey, C.W., Rogers, N.W. and Calsteren, P.W.C. (1990) Source and differentiation of Deccan Trap lavas: implications of geochemical and mineral chemical variations. Jour. Petrol., v.31, pp.1165-1200.

Liu, Q., Roberts, A.P., Larrasoaña, J.C., Banerjee, S.K., Guyodo, Y., Tauxe, L. and Oldfeld, F. (2012) Environmental magnetism: principles and applications. Rev. Geophys., v.50(4), RG4002, pp.1-50. DOI:10.1029/2012RG000393.

Mahoney, J.J. (1988) Deccan Traps. *In:* Macdougall, J.D. (Ed.), Continental flood basalts. (Dorrecht: Kluwer-Academic), pp. 151-194.

Melluso, L., Mahoney, J. J. and Dallai, L. (2006) Mantle sources and crustal input as recorded in high-Mg Deccan Traps basalts of Gujarat (India). Lithos, v.89, pp.259-274.

Michael, D.H. and Chandrasekharam, D. (2007) Nature of Sub-volcanic Magma Chambers, Deccan Province, India: Evidence from Quantitative Textural Analysis of Plagioclase Megacrysts in the Giant Plagioclase Basalts. Jour. Petrol., v.48(5), pp.885-900. doi:10.1093/petrology/egm005.

Mitchell, C. and Widdowson, M. (1991) A geological map of the southern Deccan Traps, India and its structural implications. Jour. the Geol Soc, London, v.148, pp.495-505.

Peng, Z.X., Mahoney, J.J., Hooper, P.R., Harris, C. and Beane, J.E. (1994) A role for lower continental crust in flood basalt genesis? Isotopic and incompatible element study of the lower six formations of the western Deccan traps. Geochim. Cosmochim. Acta, v.58, pp.267-288.

Peng, Z.X., Mahoney, J.J., Hooper, P.R., Macdougall, J.D. and Krishnamurthy, P. (1998) Basalts of the northeastern Deccan Traps, India: Isotopic and elemental geochemistry and relation to southwestern Deccan stratigraphy. Jour. Geophys. Res., v.103/29, pp.843-829.

Radhakrishna Murthy, C. and Likhite, S. D. (1970b) Relation between Thermal Variation of Low-field Susceptibility and Magnetic Hysteresis in Basalts. Earth Planet. Sci. Lett., v.9, pp.294-298.

Radhakrishna Murthy, C., and Deutsch, E. R. (1974) Magnetic Techniques for Ascertaining the Nature of Iron Oxide Grains in Basalts. Jour. Geophys. Res., v.40, pp.453-465.

Radhakrishnamurty, C. and Subbarao, K.V. (1990) Palaeomagnetism and rock magnetism of Deccan traps. Proc. Indian Acad. Sci. (Earth Planet. Sci.), v.99(4), ,pp.669-680.

Rahdakrishanamurty, C., Likehite, S.D. and Sahasrabhude, P.W., (1977) Nature of magnetic grains and their effects on the remanent Magnetization of basalt. Phys. Earth Planet. Inter., v.13, pp.289-300.

Radhakrishnamurty, C., Likhite, S.D., Deutsch, E.R. and Murthy, G.S. (1981) A comparison of the magnetic properties of synthetic titanomagnetities and basalts. Phys. Earth. Planet. Inter., v.26, pp.37-46.

Radhakrishnaмurthy, C. (1990) Mixed Domain States of Magnetic Grains in Basalts and Implications for Palaeomagnetism. Phys. Earth Planet. Inter., v.64, pp.348–354.

Sangode, S.J. (2014) Applications of Magnetic Stratigraphy into Quaternary Records of India. Gondwana Geol. Mag., v.29 (1 and 2), pp.67-86.

Sangode, S.J., Sharma, R., Mahajan, R., Basavaiah, N., Srivastava P., Gudadhe, S.S., Meshram, D.C., Venkateshwarulu, M. (2017) Anisotropy of Magnetic Susceptibility and Rock Magnetic Applications in the Deccan Volcanic Province based on some Case Studies. Jour. Geol. Soc. India, v.89, pp.631-642.

Sen, G. (1995) A simple petrologic model for the generation of Deccan Traps magmas. Internat. Geol. Rev., v.37, pp.825-850.

Sen, G. (2001) Generation of Deccan Trap magmas. Proc. Indian National Science Academy, v.110, pp.409-431.

Sheth, H. C. and Melluso, L. (2008) The Mount Pavagadh volcanic suite, Deccan Traps: Geochemical stratigraphy and magmatic evolution. Jour. Asian Earth Sci.s, v.32, pp.5-21.

Sparks, R.S.J. and Huppert, H.E. (1984) Density changes during the fractional crystallization of basaltic magmas: fluid dynamic implications. Contrib. Mineral. Petrol., v.85, pp.300-309.

Subbarao, K.V. and Hooper, P.R. (1988) Reconnaissance map of the Deccan Basalt Group in the Western Ghats, India; *In:* Deccan Flood Basalts. K.V. Subbarao (Ed.), Mem. Geol. Soc. India, no.10 (enclosure).

Subbarao, K.V., Chandrasekharam, D., Navaneethakrishnan, P., and Hooper, P.R. (1994) Stratigraphy and structure of parts of the central Deccan basalt province: Eruptive models. *In:* Volcanism, K.V. Subbarao (Ed.), Wiley Eastern, New Delhi, pp.321-332,

Subbarao, K.V., Bodas, M.S., Hooper, P.R. and Walsh, J.N. (1988) Petrogenesis of Jawhar and Igatpuri formations western Deccan basalt province, in Deccan Flood Basalts. K.V. Subbarao (Ed.). Mem. Geol. Soc. India, no.10, pp.253-280.

Subbarao, K.V., Bodas, M.S.,Khadri, S.F.R. and Beane, J.E. (2000) Penrose Deccan 2000, Field Excursion Guide to the Western Deccan Basalt Province. Penrose Field Guides, Geol. Soc. India, Bangalore (enclosure).

Thompson, R. and Oldfield, F. (1986) Environmental Magnetism. Allen and Unwin, Winchester, Mass., doi:10.1007/978-94-011-8036-8.